

## Biotechnology

# Identification of Amino Acid Residues Responsible for C–H Activation in Type-III Copper Enzymes by Generating Tyrosinase Activity in a Catechol Oxidase

Ioannis Kampatsikas, Matthias Pretzler, and Annette Rompel\*

**Abstract:** Tyrosinases (TYRs) catalyze the hydroxylation of phenols and the oxidation of the resulting *o*-diphenols to *o*-quinones, while catechol oxidases (COs) exhibit only the latter activity. Aurone synthase (AUS) is not able to react with classical tyrosinase substrates, such as tyramine and L-tyrosine, while it can hydroxylate its natural substrate isoliquiritigenin. The structural difference of TYRs, COs, and AUS at the heart of their divergent catalytic activities is still a puzzle. Therefore, a library of 39 mutants of AUS from *Coreopsis grandiflora* (CgAUS) was generated and the activity studies showed that the reactivity of the three conserved histidines (HisA<sub>2</sub>, HisB<sub>1</sub>, and HisB<sub>2</sub>) is tuned by their adjacent residues (HisB<sub>1</sub>+1, HisB<sub>2</sub>+1, and waterkeeper residue) either to react as stronger bases or / and to stabilize a position permissive for substrate proton shuffling. This provides the understanding for C–H activation based on the type-III copper center to be used in future biotechnological processes.

The type-III copper family includes the enzymes tyrosinase (TYR), catechol oxidase (CO) and aurone synthase (AUS), which are summarized under the umbrella term polyphenol oxidases (PPOs).<sup>[1,2]</sup> They are omnipresent among archaea, bacteria, fungi, animals and plants.<sup>[3–5]</sup> TYRs are bi-functional PPOs catalyzing the *o*-hydroxylation of monophenols (monophenolase activity, EC 1.14.18.1), which is coupled to the subsequent two-electron oxidation of the resulting *o*-diphenols to *o*-quinones (diphenolase activity, EC 1.10.3.1),<sup>[2]</sup> whereas COs exhibit only the latter diphenolase reactivity. The enzyme-in-between AUS catalyzes *in vivo* the formation of aurones and wild type AUS from *Coreopsis grandiflora* (CgAUS<sub>wt</sub>) exhibits a weak hydroxylase activity towards its natural substrate isoliquiritigenin<sup>[6]</sup>, while it does not react with the classical TYR substrates L-tyrosine and tyramine and was therefore classified as a CO.<sup>[6,7]</sup> PPOs are involved in a wide spectrum of important natural reactions from the browning of fruits<sup>[8]</sup> over the color of the animals' skin to

being involved in human diseases such as albinism,<sup>[9]</sup> melanoma<sup>[10]</sup> and neurodegenerative diseases (Parkinson).<sup>[11]</sup>

The search for the structural difference between TYRs and COs as the basis for their different catalytic activities has been going on for decades. The high similarity of the PPO's active centers from bacteria to animals has been described through 102 PDB entries covering 18 different proteins from 16 organisms (as of July 2020). The discussion about the amino acids decisive for different reactivity is summarized in recent studies.<sup>[12–16]</sup> The initial explanation for the lack of monophenolase activity in COs was the presence of a phenylalanine, the so-called gatekeeper residue atop of CuA (Figure 1) present in the sweet potato CO (*Ib*CO) structure.<sup>[17,18]</sup> However, the first crystal structure of a plant TYR from *Juglans regia* (*Jr*PPO1) did also show the presence of this bulky phenylalanine, which falsified the idea of the gatekeeper residue as blocking substrate access.<sup>[19]</sup> A more recent theory claims that the deprotonation of the monophenolic substrate and consequently the tyrosinase activity originates from a highly conserved water molecule (Figure 1) which is stabilized by an asparagine (HisB<sub>1</sub>+1) adjacent to

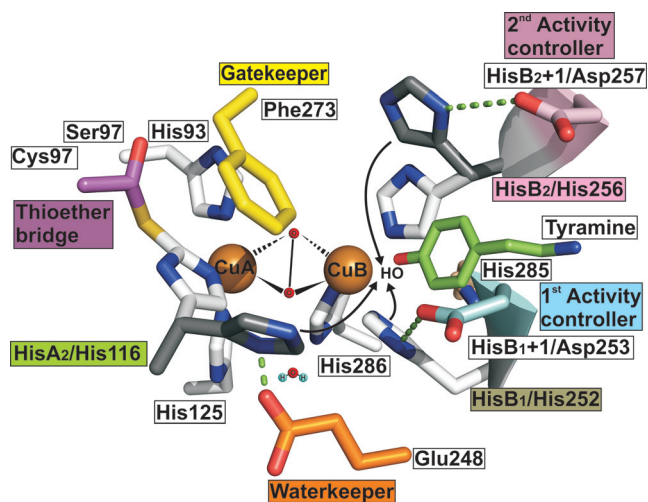


**Figure 1.** Active center of CgAUS (Cys97Ser/Thr253Asp/Arg257Asp) mutant. The mutated activity controllers Asp253 (cyan, HisB<sub>1</sub>+1), Asp257 (violet, HisB<sub>2</sub>+1), the thioether bridge constituent Cys97 (lilac, Ser97 in the mutant), the gatekeeper residue Phe273 (yellow) and the waterkeeper residue Glu248 (orange) are highlighted. The six conserved histidines His93 (HisA<sub>1</sub>), His116 (HisA<sub>2</sub>) and His125 (HisA<sub>3</sub>) of CuA and His252 (HisB<sub>1</sub>), His256 (HisB<sub>2</sub>), and His286 (HisB<sub>3</sub>) of CuB are depicted (carbon atoms in white and nitrogen atoms in blue). The 7<sup>th</sup> His285 is depicted (wheat colored) and the water next to Glu248 represents the conserved water modelled into a number of high-resolution crystal structures.

[\*] Dr. I. Kampatsikas, Dipl.-Ing. M. Pretzler, Prof. A. Rompel  
Universität Wien, Fakultät für Chemie, Institut für Biophysikalische  
Chemie  
Althanstraße 14, 1090 Wien (Austria)  
E-mail: annette.rompel@univie.ac.at  
Homepage: <https://www.bpc.univie.ac.at>

Supporting information and the ORCID identification number(s) for the author(s) of this article can be found under:  
<https://doi.org/10.1002/anie.202008859>.

© 2020 The Authors. Published by Wiley-VCH GmbH. This is an open access article under the terms of the Creative Commons Attribution License, which permits use, distribution and reproduction in any medium, provided the original work is properly cited.

the first CuB coordinating histidine (HisB<sub>1</sub>) and activated by a conserved glutamate, the so-called waterkeeper residue (Figure 1).<sup>[14]</sup> However, the asparagine residue at HisB<sub>1</sub> + 1 cannot be the solely responsible amino acid, as tyrosinase activity towards the classical substrates has been demonstrated for mushroom *AbPPO4*,<sup>[20]</sup> apple (*MdPPO1* and *MdPPO3*),<sup>[13,21,22]</sup> *Larrea tridentata* PPO<sup>[23]</sup> and tomato *SPPPO1*,<sup>[24]</sup> which all do not contain an asparagine at HisB<sub>1</sub> + 1. Recently, two non-conserved amino acids placed next to the conserved first (HisB<sub>1</sub> + 1, Thr253 in *CgAUS<sub>wt</sub>*) and second histidine (HisB<sub>2</sub> + 1, Arg257 in *CgAUS<sub>wt</sub>*) residues coordinating CuB, have been identified and termed activity controllers, both being located on an  $\alpha$ -helix in front of the PPO's catalytic center (Figure 1).<sup>[12a,13]</sup> Mutagenesis studies on *JrPPO1* and *Taraxacum officinale* PPOs (*ToPPO2*, a TYR and *ToPPO6*, a CO) proved the influence of these amino acid residues on tyrosinase activity.<sup>[15,16]</sup> However, until now no study reported the generation of hydroxylase activity in a CO.

The numerous published crystal structures of type-III copper proteins and the considerably smaller number of mutation studies have not yet elucidated the cause for hydroxylase activity in type-III copper enzymes and thus, a different approach to tackle this puzzling question is necessary. Therefore, we established a library of 39 *CgAUS* mutants that focus on residues next to the conserved histidines (HisA<sub>2</sub>, HisB<sub>1</sub> and HisB<sub>2</sub>) which are in close proximity to the substrate, that is, those in front of the active center (Figure 1). Similarly, previous studies converted the activity mode of the investigated enzymes using them as scaffolds (e.g. esterase to aldolase, esterase to epoxide hydrolase and the investigations between phenylalanine and tyrosine ammonia lyases-mutases).<sup>[25–27]</sup> Moreover, mutations targeting the residues gatekeeper (Phe273), waterkeeper (Glu248), the 7<sup>th</sup> histidine (His285) and two cysteines (Cys31 and Cys32) forming the conserved disulfide bonds (Figures S1 and S2) are summarized in the SI. The *CgAUS* mutants were heterologously expressed in *E. coli*,

purified to homogeneity (Figure S3) and tested towards reactivity with the classical monophenolic substrates tyramine (Figure S4) and L-tyrosine (Figure S5) and the corresponding diphenols dopamine (Figure S6) and L-Dopa (Figure S7). For tyramine and dopamine the  $K_m$  and  $k_{cat}$  values were determined and the mutants' copper content was measured colorimetrically. The mutants' ability to form an *oxy*-adduct has been investigated (Table 1, Table S1). All publicly avail-

**Table 1:** Measurements of the copper content (percentage based on 2 copper ions per active center),  $k_{cat}$  and  $K_m$  values with dopamine and tyramine and the absorption coefficient at  $\lambda = 345$  nm after the titration of the mutants with H<sub>2</sub>O<sub>2</sub>. Mutations which failed to create a peak at 345 nm after the incubation with H<sub>2</sub>O<sub>2</sub> are presented as “–” and “nd” indicates no detected activity.

| Mutants   | Copper %   | Dopamine $k_{cat}$ [s <sup>-1</sup> ] | $K_m$ [mM]  | Tyramine $k_{cat}$ [s <sup>-1</sup> ] | $K_m$ [mM]  | H <sub>2</sub> O <sub>2</sub> $\epsilon_{345}$ [M <sup>-1</sup> cm <sup>-1</sup> ] |
|---|------------|---------------------------------------|-------------|---------------------------------------|-------------|--|
| <i>CgAUS<sub>wt</sub></i>   | 46.1 ± 1.0 | 556 ± 27.2                            | 8.63 ± 0.28 | nd                                    | nd          | 5190   |
| Thioether bridge constituent  |            |                                       |             |                                       |             |  |
| Cys97Ala  | 42.4 ± 1.4 | 5.84 ± 0.31                           | 1.59 ± 0.09 | 0.14 ± 0.01                           | 3.03 ± 0.18 | –  |
| Cys97Gly  | 34.1 ± 2.3 | 43 ± 2.5                              | 7.53 ± 0.45 | 0.12 ± 0.01                           | 2.96 ± 0.16 | –  |
| Cys97Asp  | 52.7 ± 0.6 | 1.54 ± 0.07                           | 1.68 ± 0.07 | 0.07 ± 0.00                           | 1.05 ± 0.02 | –  |
| Cys97Asn  | 45.7 ± 0.6 | 1.24 ± 0.06                           | 0.80 ± 0.05 | 0.05 ± 0.00                           | 2.11 ± 0.08 | –  |
| Cys97Ser  | 59.3 ± 0.5 | 15 ± 1.26                             | 1.26 ± 0.04 | 0.55 ± 0.04                           | 3.59 ± 0.33 | 7600   |
| HisB <sub>1</sub> + 1 (1 <sup>st</sup> activity controller residue)   |            |                                       |             |                                       |             |  |
| Thr253Asp   | 45.0 ± 0.9 | 530 ± 33.7                            | 1.93 ± 0.12 | 2.14 ± 0.16                           | 30.9 ± 7.27 | 3800   |
| Thr253Asn   | 83.6 ± 2.5 | 850 ± 46.5                            | 4.99 ± 0.38 | 1.19 ± 0.14                           | 11.5 ± 2.69 | 19840  |
| Thr253Glu   | 46.7 ± 5.2 | 1394 ± 90.7                           | 3.59 ± 0.22 | 0.21 ± 0.02                           | 11.5 ± 1.06 | 7490   |
| Thr253Gly   | 72.8 ± 0.9 | 337 ± 24.3                            | 8.74 ± 0.92 | 0.07 ± 0.00                           | 2.22 ± 0.14 | 8600   |
| Thr253Ser   | 52.7 ± 0.0 | 500 ± 29.0                            | 6.62 ± 0.37 | 0.01 ± 0.00                           | 1.18 ± 0.09 | 8570   |
| Thr253Cys   | 56.9 ± 1.8 | 312 ± 14.8                            | 11.1 ± 0.33 | 0.04 ± 0.00                           | 4.32 ± 0.28 | 14220  |
| Thr253Ala   | 56.1 ± 3.2 | 140 ± 7.2                             | 5.80 ± 0.30 | 0.05 ± 0.00                           | 1.48 ± 0.04 | 7850   |
| Thr253Ile   | 58.2 ± 0.8 | 27 ± 1.1                              | 13.6 ± 0.72 | nd                                    | nd          | 9980   |
| Thr253Lys   | 4.8 ± 0.8  | 20 ± 3.2                              | 38.6 ± 7.88 | nd                                    | nd          | –  |
| HisB <sub>2</sub> + 1 (2 <sup>nd</sup> activity controller residue)   |            |                                       |             |                                       |             |  |
| Arg257Asp   | 11.1 ± 0.8 | 1380 ± 95.3                           | 1.26 ± 0.13 | 8.26 ± 0.48                           | 4.01 ± 0.29 | 10470  |
| Arg257Leu   | 64.5 ± 2.1 | 2245 ± 125                            | 5.91 ± 0.25 | nd                                    | nd          | 14890  |
| Arg257Ile   | 66.3 ± 1.2 | 1660 ± 93.6                           | 3.57 ± 0.17 | nd                                    | nd          | 11060  |
| Arg257Gly   | 79.6 ± 1.8 | 1264 ± 63.7                           | 3.54 ± 0.26 | nd                                    | nd          | 3490   |
| HisB <sub>1</sub> + 1 and HisB <sub>2</sub> + 1 (1 <sup>st</sup> and 2 <sup>nd</sup> activity controllers) and thioether bridge constituent |            |                                       |             |                                       |             |  |
| Thr253Asp   | 43.5 ± 1.7 | 171 ± 10.2                            | 0.24 ± 0.02 | 9.48 ± 0.55                           | 1.09 ± 0.09 | 4570   |
| Arg257Asp   |            |                                       |             |                                       |             |  |
| Thr253Asp   | 32.8 ± 0.4 | 662 ± 30.0                            | 1.31 ± 0.04 | 1.91 ± 0.11                           | 4.59 ± 0.25 | 8610   |
| Arg257Gly   |            |                                       |             |                                       |             |  |
| Thr253Gly   | 33.8 ± 0.8 | 535 ± 39.9                            | 4.00 ± 0.46 | 0.05 ± 0.00                           | 0.75 ± 0.07 | 7690   |
| Arg257Leu   |            |                                       |             |                                       |             |  |
| Thr253Ser   | 33.0 ± 0.0 | 430 ± 26.1                            | 2.37 ± 0.26 | 0.01 ± 0.00                           | 0.73 ± 0.10 | 5660   |
| Arg257Gly   |            |                                       |             |                                       |             |  |
| Thr253Gly   | 52.1 ± 0.4 | 859 ± 52.9                            | 1.29 ± 0.09 | 0.02 ± 0.00                           | 0.46 ± 0.03 | 15990  |
| Arg257Val   |            |                                       |             |                                       |             |  |
| Thr253Gly   | 10.6 ± 1.6 | 191 ± 9.11                            | 2.09 ± 0.09 | 0.56 ± 0.03                           | 15.5 ± 1.03 | 2620   |
| Arg257Thr   |            |                                       |             |                                       |             |  |
| Cys97Ser  | 40.2 ± 0.6 | 19 ± 1.22                             | 0.06 ± 0.00 | 6.52 ± 0.39                           | 0.02 ± 0.00 | 3700   |
| Thr253Asp   |            |                                       |             |                                       |             |  |
| Arg257Asp   |            |                                       |             |                                       |             |  |

able crystal structures of type-III copper enzymes have been taken into consideration to interpret our data.

**Mutations next to the conserved His<sub>B1</sub> residue (1<sup>st</sup> activity controller position):** Nine (Asp, Asn, Glu, Gly, Ser, Cys, Ala, Ile and Lys) mutants have been produced targeting the non-conserved His<sub>B1</sub>+1 residue (called 1<sup>st</sup> activity controller; Thr253 in *CgAUS<sub>wt</sub>*), and were examined with regard to their hydroxylase activity against tyramine (Table 1 and Figure S4). The tyramine reaction rates of Thr253Asp, Thr253Asn and Thr253Glu featuring either a (deprotonated) carboxylic acid (Asp and Glu) or a carboxamide (Asn) were particularly high ( $k_{\text{cat}} = 2.14, 1.19$  and  $0.21 \text{ s}^{-1}$ , respectively) and notably of the same order of magnitude as seen in natural plant TYRs like apple *MdPPO1-3* ( $k_{\text{cat}} = 9.5, 0.92$  and  $1.0 \text{ s}^{-1}$ , respectively).<sup>[13]</sup> The mutants Thr253Gly, Thr253Ser, Thr253Cys and Thr253Ala exhibit significantly lower  $k_{\text{cat}}$  values but undoubtedly showed hydroxylase activity, while Thr253Ile and Thr253Lys did not induce monophenolase activity and remained COs (Table 1). The amino acid residues His252

and its neighbor one 253 are relatively close to each other (2.8 Å in *CgAUS<sub>wt</sub>* His252-Thr253, PDB: 4Z14) due to the turn of the  $\alpha$ -helix (Figure S8). The higher hydroxylase activity in Thr253Asp, Thr253Asn and Thr253Glu is explained by hydrogen bonds which the amino acid residues at position 253 can form with the His252 (His<sub>B1</sub>+1), and which increase the basicity of the conserved His252. Thus, the incoming monophenolic substrates will be deprotonated by His252 which serves as a base (Figure 2). The faster hydroxylation rate of Thr253Asp over Thr253Glu (2.14 vs.  $0.21 \text{ s}^{-1}$ ) indicates the importance of the precise activating amino acid side chain position of the His<sub>B1</sub>+1 residue. Glutamic acid with its additional CH<sub>2</sub> group is 4.7 Å away from His<sub>B1</sub> showing a weaker hydrogen bond interaction than Asp253 or Asn253 at a distance of 2.6 and 2.8 Å, respectively (Figure S9). Interactions between Asp or Asn with His are similar to catalytic triads as described in the well-characterized proteases chymotrypsin (PDB: 4H4F) Asp102-His57-Ser195 (acid-base-nucleophile) and papain (PDB: 1PPN)

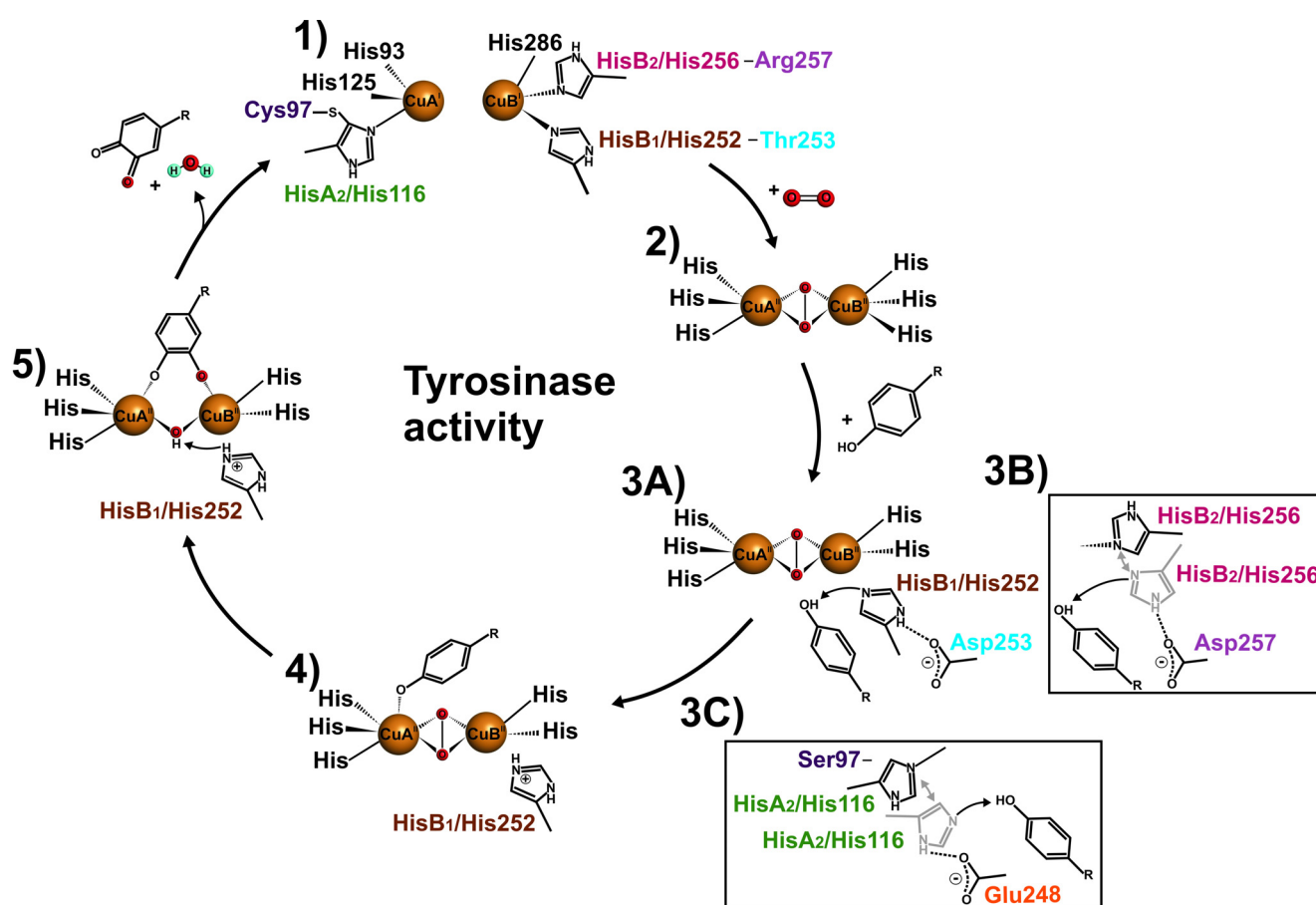


**Figure 2.** Tyrosinase activity of type-III copper enzymes. **1)** The deoxy-form of type-III copper centers (Cu<sup>I</sup>-Cu<sup>I</sup>) binds molecular oxygen and thereby transitions to the catalytically competent oxy-form (Cu<sup>II</sup>-Cu<sup>II</sup>). **2)** Three of the six conserved histidines (His<sub>A2</sub>, His<sub>B1</sub>, and His<sub>B2</sub>) are responsible for the deprotonation of the incoming monophenolic substrate. **3A)** In the Thr253Asp mutant His<sub>B1</sub>'s basicity is increased by the adjacent amino acid residue Asp253 (His<sub>B1</sub>+1) which can enhance the deprotonation of the incoming substrate. **3B)** Similarly, in the Arg257Asp mutant His<sub>B2</sub> approaches Asp257 (His<sub>B2</sub>+1) and becomes more basic. **3C)** In the Cys97Ser mutant His<sub>A2</sub> is released by the severing of the thioether bridge and thus is flexible enough to approach the waterkeeper residue Glu248, become more basic and deprotonate the incoming substrate. **4)** The deprotonated monophenol is now susceptible to catalytically productive interaction with the oxy-form of the type-III copper center. **5)** *Ortho*-Hydroxylation of the phenolate proceeds via electrophilic aromatic substitution, and subsequent two-electron oxidation yields an *ortho*-quinone and water. These two electrons reduce the type-III copper center to its *deoxy*-form, thereby closing the catalytic cycle.

Asn175-His159-Cys25 (stabilizer-base-nucleophile, Figure S10).<sup>[28]</sup> Transient Schiff base formation and glutamate-supported proton transfer during catalysis have been reported for many reaction mechanisms, for example for aldolases.<sup>[29–31]</sup>

**Mutations next to the conserved HisB<sub>2</sub> residue (2<sup>nd</sup> activity controller position):** Out of the four mutants (Asp, Leu, Ile and Gly) targeting the HisB<sub>2</sub>+1 (2<sup>nd</sup> activity controller) residue only Arg257Asp gained tyrosinase activity with an intriguing turnover rate ( $k_{\text{cat}} = 8.26 \text{ s}^{-1}$ ). The generation of monophenolase activity in Arg257Asp is caused by the replacement of the positively charged Arg257 residue in CgAUS<sub>wt</sub> with the negatively charged Asp257 which enhances the basicity of His256 (HisB<sub>2</sub>) similar to activation of His252 (HisB<sub>1</sub>) by Asp253. However, the side chain of Asp257 is 6.3 Å apart from the conserved His256, and thus, cannot directly influence the basic potential of the conserved His256 from this position. Notwithstanding, the distances mentioned are not to be understood absolutely, as a great deal of flexibility of the two copper ions CuA and CuB, and thus the conserved histidines, has been described several times in PPOs as a prerequisite for functionality.<sup>[32,33]</sup> According to this flexibility of the conserved His, His256 can come closer to Asp257 (2.6 Å) and make a hydrogen bond, forming the charge-relay network to deprotonate the incoming substrate (Figure S11).

**Double mutants at the HisB<sub>1</sub>+1 and HisB<sub>2</sub>+1 residues (1<sup>st</sup> and 2<sup>nd</sup> activity controllers):** The Thr253Asp/Arg257Gly, Thr253Gly/Arg257Leu and Thr253Gly/Arg257Thr mutants mimicked the characterized and verified TYRs *AbPPO4*,<sup>[34]</sup> *LtPPO*<sup>[23]</sup> and *MdPPO3*<sup>[13]</sup> matching their respective activity controller combinations and all three double mutants are endowed with tyrosinase activity (Table 1). Based on the results obtained for the single mutants at the HisB<sub>1</sub>+1 and HisB<sub>2</sub>+1 residues the double mutant Thr253Asp/Arg257Asp is expected to be the strongest TYR and does indeed show the highest reaction rate on tyramine ( $k_{\text{cat}} = 9.48 \text{ s}^{-1}$ , Table 1) showing that the negatively charged aspartic acids at the activity controllers' positions provide so far maximal tyrosinase activity.

**The thioether bridge between the cysteine sulfur and the conserved HisA<sub>2</sub> residue:** CgAUS<sub>wt</sub> contains a thioether bridge between the cysteine sulfur (Cys97) and the Cε of the conserved HisA<sub>2</sub> (His116, see Figure 1). This bond fixates the conserved HisA<sub>2</sub> and is proposed to support electron transfer.<sup>[18,19]</sup> The thioether bridge is a conserved feature in plant and fungal PPOs,<sup>[7,13,33]</sup> whereas it is normally absent in bacteria and mammals (Figure S12).<sup>[14]</sup> Five mutants (Ala, Gly, Asp, Asn and Ser) that replace Cys97 were produced to prevent thioether bond formation. All five mutants show hydroxylase activity (Table 1), which presumably originates from the release of HisA<sub>2</sub> from the thioether bridge (Figure 1).<sup>[32]</sup> Mutants lacking the thioether linkage allow HisA<sub>2</sub> to approach the entrance of the dicopper center and act as a base and additionally increase its basicity by interacting with the conserved waterkeeper residue Glu248 (Figure 1). The triple mutant Cys97Ser/Thr253Asp/Arg257Asp targeting the three main positions examined in this work (Figure 1), showed a lower activity rate on tyramine ( $k_{\text{cat}} = 6.52 \text{ s}^{-1}$ ) compared to the double mutant Thr253Asp/Arg257Asp

( $9.48 \text{ s}^{-1}$ , Table 1) which suggests that HisA<sub>2</sub> does not add significantly to the deprotonation of the substrate caused by HisB<sub>1</sub> and HisB<sub>2</sub>. Although not faster, the catalytic efficiency of the mutant Cys97Ser/Thr253Asp/Arg257Asp was  $\approx 326 \text{ s}^{-1} \text{ mM}^{-1}$  compared to Thr253Asp/Arg257Asp with  $\approx 8.7 \text{ s}^{-1} \text{ mM}^{-1}$  due to the high specificity of the triple mutant for tyramine ( $K_{\text{m}} = 0.02 \text{ mM}$ , Table 1).

**The gatekeeper residue (Phe273), waterkeeper residue (Glu248), 7<sup>th</sup> His residue (His285), Cys31 and Cys32 residues:** This study also reports on mutants addressing the gatekeeper residue (Phe273), waterkeeper residue (Glu248), 7<sup>th</sup> His residue (His285), Cys31 and Cys32 residues. Some of them have a minor influence on C–H activation, but exert a significant influence on the total activity of the enzyme, which in most cases is impaired (see SI).

**Flexibility of the conserved histidines facing the substrate as a prerequisite for C–H activation in type-III copper centers:** In PPOs, the flexibility of the two copper ions is high as supported by crystallographic data obtained from different enzymatic stages (*oxy*, *met* and *deoxy*). The structures of *oxy* (PDB: 4Z13) and *deoxy* (PDB: 4Z14) CgAUS exhibit a difference of  $\approx 1 \text{ Å}$  in the copper-copper distance. Upon formation of the *oxy*-form both copper atoms move from the initial *deoxy* copper position, CuA by 0.5 Å and CuB by 0.7 Å.<sup>[7]</sup> Recently, Matoba *et al.* investigated the bacterial TYR from *Streptomyces castaneoglobisporus* and showed that the flexibility of the two Cu ions has an impact on the position of the conserved histidines.<sup>[32]</sup> Moreover, Fujieda *et al.* show a similar influence of copper ion flexibility on conserved His of *Aspergillus oryzae* TYR and based on crystallographic studies proposed that the deprotonation of the substrate probably happens by HisA<sub>3</sub> (His103) because of its lost interactions with CuA during substrate approach.<sup>[35]</sup> Furthermore, the crystal structure of active mushroom TYR *AbPPO4*<sup>[33]</sup> revealed two CuB conformations with 2.3 Å distance between them. The second CuB position shows interaction with a fourth imidazole group (three with the conserved histidines and one additional with the 7<sup>th</sup> histidine). Therefore, in *AbPPO4*, the 7<sup>th</sup> histidine can react as a backup residue and supports the flexibility of the copper ion and histidines.<sup>[33]</sup> All of this reveals that PPOs contain a flexible dicopper center where the two copper ions can occupy different positions and consequently the conserved histidines are available for the additional task of substrate deprotonation besides copper coordination.

**Formation of the oxy-complex as the primary step in the monophenolase cycle:** All CgAUS mutants were titrated with H<sub>2</sub>O<sub>2</sub> and their conversion to the *oxy*-form was investigated by determining the  $\epsilon_{345}$  absorption coefficient (Table 1 and S1) and the number of equivalents needed for saturation (Table S1). All mutants targeting the HisB<sub>1</sub>+1 and HisB<sub>2</sub>+1 (Thr253 and Arg257) residues which exhibited monophenolase activity did also form an *oxy*-adduct. Mutants Thr253Ile, Arg257Leu and Arg257Ile were unable to hydroxylate monophenolic substrates although showing a strong *oxy*-adduct induced by H<sub>2</sub>O<sub>2</sub> (Table S1). Hence, the ability of PPOs to form a stable *oxy*-adduct represents merely the first step in the monophenolase cycle (Figure 2).

*Monophenolase cycle for type-III copper enzymes (Figure 2): Deoxy-CgAUS (Cu<sup>I</sup>) binds molecular oxygen and forms the oxy-form (Cu<sup>II</sup>) (1→2). The incoming monophenolic substrate needs to be deprotonated, which is supported by one of the three conserved histidines HisA<sub>2</sub>, HisB<sub>1</sub> and HisB<sub>2</sub> en route to the active oxy-site (2→3A, 3B and 3C). Due to the flexibility of the two copper ions the detached histidines serve as bases (3). The reactivity of the three histidines (HisA<sub>2</sub>, HisB<sub>1</sub> and HisB<sub>2</sub>) is tuned by their adjacent residues (HisB<sub>1</sub>+1, HisB<sub>2</sub>+1 and waterkeeper residue) either to react as stronger bases or / and to stabilize a position suitable for substrate proton shuffling (3). The deprotonated substrate binds to CuA<sup>[32]</sup> or in the middle of the two copper ions<sup>[7]</sup> resulting in hydroxylation (4). The dicopper center converts to the met-form after transferring one oxygen atom to the substrate (5) and the oxidation of the diphenolic substrate leads to the final quinone product while the enzyme returns to the deoxy-form for a new catalytic cycle (5→1).*

**Implications:** Firstly, the residues that control the substrate specificity in type-III copper proteins have been identified. The type of amino acids present at these positions causes the disparity of the structurally similar TYRs and COs. Secondly, we demonstrated how a CO type enzyme can be converted to a TYR by mutating the residues HisB<sub>1</sub>+1, HisB<sub>2</sub>+1 or the Cys of the thioether bridge. Finally, our findings contribute to the basic understanding of the monophenolase reaction cycle (Figure 2). The present study explains for the first time that hydroxylase activity in type-III copper enzymes is a result of the flexibility of the three conserved HisA<sub>2</sub>, HisB<sub>1</sub> and HisB<sub>2</sub>, allowing them to act as bases and deprotonate monophenolic substrates initiating the C–H activation in TYRs, in contrast to COs. The control of the C–H activation reaction will fundamentally impact several important applications in the fields of medicine (melanoma), biotechnology, bioremediation, post-harvest technology, textile technology, wine production and others which are of utmost importance.

## Acknowledgements

The research was funded by the Austrian Science Fund (FWF): P25217 and P32326 as well as the University of Vienna. We thank Rosa Heydenreich, B. Sc. for her support during protein expression.

## Conflict of interest

The authors declare no conflict of interest.

**Keywords:** biotechnology · C–H activation · enzyme engineering · hydroxylase versus oxidase activity · polyphenol oxidases

- [1] E. I. Solomon, D. E. Heppner, E. M. Johnston, J. W. Ginsbach, J. Cirera, M. Qayyum, M. T. Kieber-Emmons, C. H. Kjaergaard, R. G. Hadt, L. Tian, *Chem. Rev.* **2014**, *114*, 3659–3853.
- [2] C. Kaintz, S. G. Mauracher, A. Rompel, in *Adv. Protein Chem. Struct. Biol.* (Ed.: C. Z. Christov), Academic Press, San Diego, **2014**, pp. 1–35.
- [3] A. M. Mayer, *Phytochemistry* **2006**, *67*, 2318–2331.
- [4] C. Kaintz, C. Molitor, J. Thill, I. Kampatsikas, C. Michael, H. Halbwirth, A. Rompel, *FEBS Lett.* **2014**, *588*, 3417–3426.
- [5] M. Pretzler, A. Bijelic, A. Rompel, in *Ref. Module Chem. Mol. Sci. Chem. Eng.*, Elsevier, Amsterdam, **2015**, <https://doi.org/10.1016/B978-0-12-409547-2.11521-5>.
- [6] C. Molitor, S. G. Mauracher, S. Pargan, R. L. Mayer, H. Halbwirth, A. Rompel, *Planta* **2015**, *242*, 519–537.
- [7] C. Molitor, S. G. Mauracher, A. Rompel, *Proc. Natl. Acad. Sci. USA* **2016**, *113*, E1806–E1815.
- [8] A. Derardja, M. Pretzler, I. Kampatsikas, M. Barkat, A. Rompel, *Food Chem. X* **2019**, *4*, 100053.
- [9] M. B. Dolinska, N. Kus, K. Farney, P. T. Wingfield, B. P. Brooks, Y. V. Sergeev, *Pigment Cell Melanoma Res.* **2017**, *30*, 41–52.
- [10] J. L. Boyle, H. M. Haupt, J. B. Stern, H. A. B. Mulhaupt, *Arch. Pathol. Lab. Med.* **2002**, *126*, 816–822.
- [11] A. Bose, G. A. Petsko, D. Eliezer, *J. Parkinson's Dis.* **2018**, *8*, 385–398.
- [12] a) M. Pretzler, A. Rompel, *Inorg. Chim. Acta* **2018**, *481*, 25–31; b) H. Decker, E. Solem, F. Tuzcek, *Inorg. Chim. Acta* **2018**, *481*, 32–37.
- [13] I. Kampatsikas, A. Bijelic, M. Pretzler, A. Rompel, *Sci. Rep.* **2017**, *7*, 8860.
- [14] M. Goldfeder, M. Kanteev, S. Isaschar-Ovdat, N. Adir, A. Fishman, *Nat. Commun.* **2014**, *5*, 4505.
- [15] S. M. Prexler, M. Frassek, B. Moerschbacher, M. E. Dirks-Hofmeister, *Angew. Chem. Int. Ed.* **2019**, *58*, 8757–8761; *Angew. Chem.* **2019**, *131*, 8849–8853.
- [16] F. Panis, I. Kampatsikas, A. Bijelic, A. Rompel, *Sci. Rep.* **2020**, *10*, 1659.
- [17] K. A. Magnus, B. Hazes, H. Ton-That, C. Bonaventura, J. Bonaventura, W. G. J. Hol, *Proteins Struct. Funct. Bioinf.* **1994**, *19*, 302–309.
- [18] T. Klabunde, C. Eicken, J. C. Sacchettini, B. Krebs, *Nat. Struct. Mol. Biol.* **1998**, *5*, 1084–1090.
- [19] A. Bijelic, M. Pretzler, C. Molitor, F. Zekiri, A. Rompel, *Angew. Chem. Int. Ed.* **2015**, *54*, 14677–14680; *Angew. Chem.* **2015**, *127*, 14889–14893.
- [20] S. G. Mauracher, C. Molitor, C. Michael, M. Kragl, A. Rizzi, A. Rompel, *Phytochemistry* **2014**, *99*, 14–25.
- [21] I. Kampatsikas, A. Bijelic, M. Pretzler, A. Rompel, *Acta Crystallogr. Sect. F* **2017**, *73*, 491–499.
- [22] I. Kampatsikas, A. Bijelic, M. Pretzler, A. Rompel, *Angew. Chem. Int. Ed.* **2019**, *58*, 7475–7479; *Angew. Chem.* **2019**, *131*, 7553–7557.
- [23] H. J. Martin, I. Kampatsikas, R. Oost, M. Pretzler, E. Al-Sayed, A. Roller, G. Giester, A. Rompel, N. Maulide, *Chem. Eur. J.* **2018**, *24*, 15756–15760.
- [24] I. Kampatsikas, A. Bijelic, A. Rompel, *Sci. Rep.* **2019**, *9*, 4022.
- [25] M. Svedendahl, K. Hult, P. Berglund, *J. Am. Chem. Soc.* **2005**, *127*, 17988–17989.
- [26] H. Jochens, K. Stiba, C. Savile, R. Fujii, J.-G. Yu, T. Gerassenkov, R. J. Kazlauskas, U. T. Bornscheuer, *Angew. Chem. Int. Ed.* **2009**, *48*, 3532–3535; *Angew. Chem.* **2009**, *121*, 3584–3587.
- [27] S. Bartsch, U. T. Bornscheuer, *Angew. Chem. Int. Ed.* **2009**, *48*, 3362–3365; *Angew. Chem.* **2009**, *121*, 3412–3415.
- [28] T. Klein, U. Eckhard, A. Dufour, N. Solis, C. M. Overall, *Chem. Rev.* **2018**, *118*, 1137–1168.
- [29] C. Zeymer, R. Zschoche, D. Hilvert, *J. Am. Chem. Soc.* **2017**, *139*, 12541–12549.

- [30] V. Sautner, M. M. Friedrich, A. Lehweß-Litzmann, K. Tittmann, *Biochemistry* **2015**, *54*, 4475–4486.
- [31] L. Giger, S. Caner, R. Obexer, P. Kast, D. Baker, N. Ban, D. Hilvert, *Nat. Chem. Biol.* **2013**, *9*, 494–498.
- [32] Y. Matoba, S. Kihara, N. Bando, H. Yoshitsu, M. Sakaguchi, K. Kayama, S. Yanagisawa, T. Ogura, M. Sugiyama, *PLOS Biol.* **2018**, *16*, e3000077.
- [33] S. G. Mauracher, C. Molitor, R. Al-Oweini, U. Kortz, A. Rompel, *Acta Crystallogr. Sect. D* **2014**, *70*, 2301–2315.
- [34] M. Pretzler, A. Bijelic, A. Rompel, *Sci. Rep.* **2017**, *7*, 1810.
- [35] N. Fujieda, K. Umakoshi, Y. Ochi, Y. Nishikawa, S. Yanagisawa, M. Kubo, G. Kurisu, S. Itoh, *Angew. Chem. Int. Ed.* **2020**, *59*, 13385–13390; *Angew. Chem.* **2020**, *132*, 13487–13492.

Manuscript received: June 25, 2020

Accepted manuscript online: July 23, 2020

Version of record online: September 9, 2020